

Supplementary Materials

New In Situ Catalysts Based on Nitro Functional Pyrazole Derivatives and Copper (II) Salts for Promoting Oxidation of Catechol to *o*-Quinone

Abderrahim Titi ^{1,*}, Kaoutar Zaidi ¹, Abdullah Y. A. Alzahrani ², Mohamed El Kodadi ^{1,3}, El Bekkaye Yousfi ^{1,4}, Anna Moliterni ⁵, Belkheir Hammouti ¹, Rachid Touzani ^{1,*} and Mohamed Abboud ^{6,*}

¹ Laboratory of Applied and Environmental Chemistry (LCAE), Faculty of Sciences, University Mohammed Premier, Oujda 60000, Morocco; zaidikaoutar96@gmail.com (K.Z.); elkodadim@yahoo.fr (M.E.K.); yousfi@netcourrier.com (E.B.Y.); hammoutib@gmail.com (B.H.)

² Department of Chemistry, Faculty of Science and Arts, King Khalid University, Mohail Assir 62529, Saudi Arabia; ayalzahrani@kku.edu.sa

³ Laboratoire d'Innovation en Sciences, Technologie et Education (LISTE), CRMEF, Oujda 60000, Morocco

⁴ Higher Institute of Nursing and Health Professions Techniques (ISPITS), Oujda 60000, Morocco

⁵ Instituto di Cristallografia, CNR, Via Amendola, 122/0, 70126 Bari, Italy; annagrazia.moliterni@ic.cnr.it

⁶ Catalysis Research Group (CRG), Department of Chemistry, College of Science, King Khalid University, P.O. Box 9004, Abha 61413, Saudi Arabia

* Correspondence: titi_abderrahim1718@ump.ac.ma (A.T.); r.touzani@ump.ac.ma (R.T.); mabboud@kku.edu.sa (M.A.)

1. Characterization

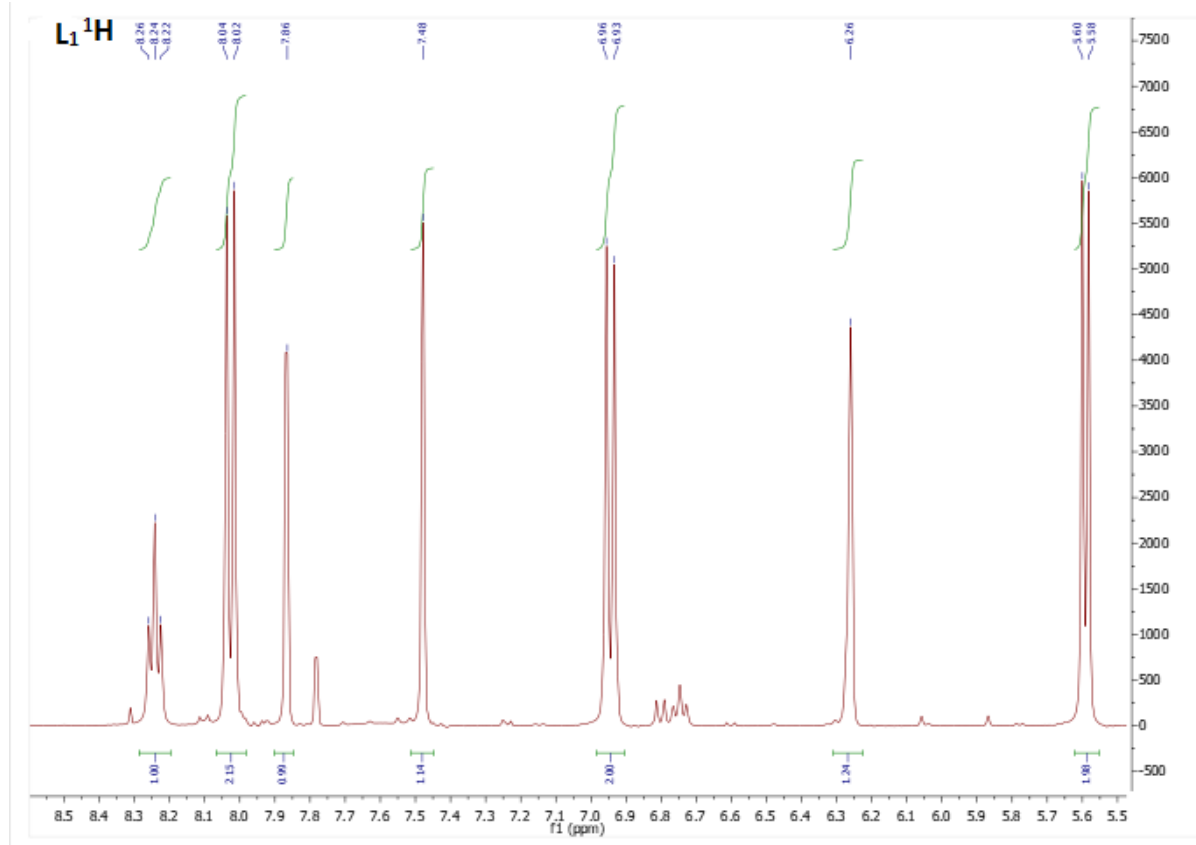


Figure S1. ¹H NMR spectrum of L1 in DMSO (400 MHz).

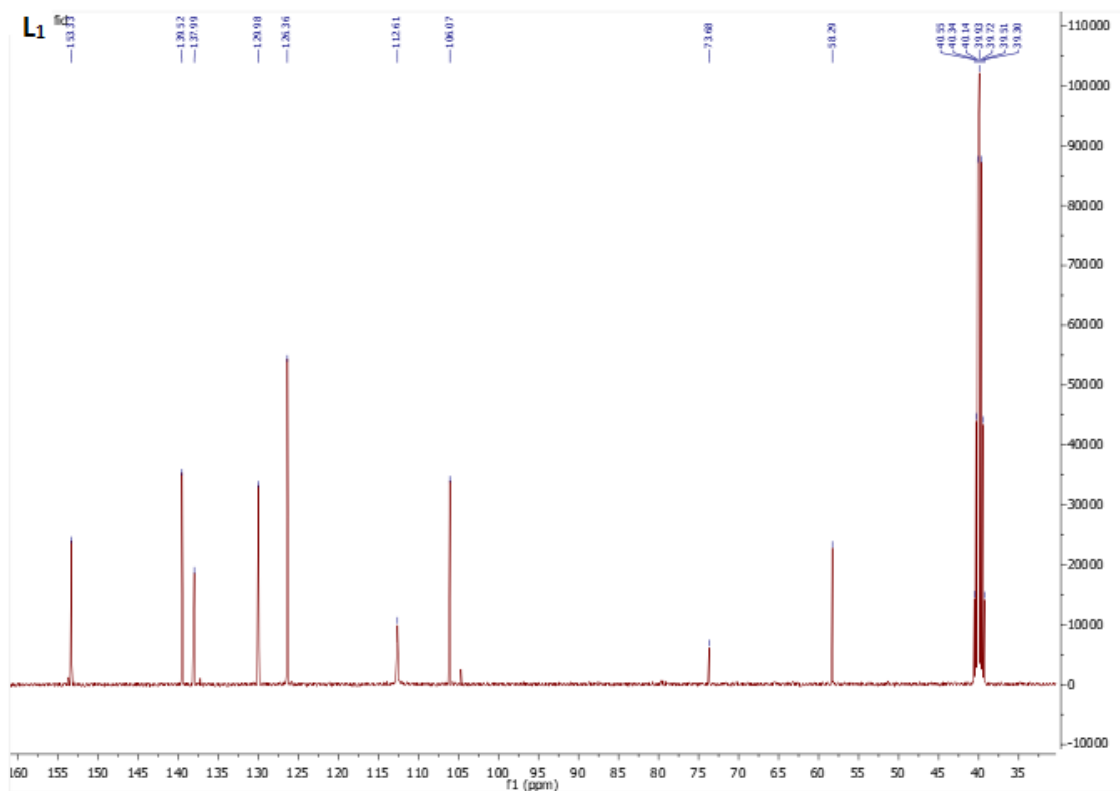


Figure S2. ^{13}C NMR spectrum of L_1 in DMSO (400 MHz).

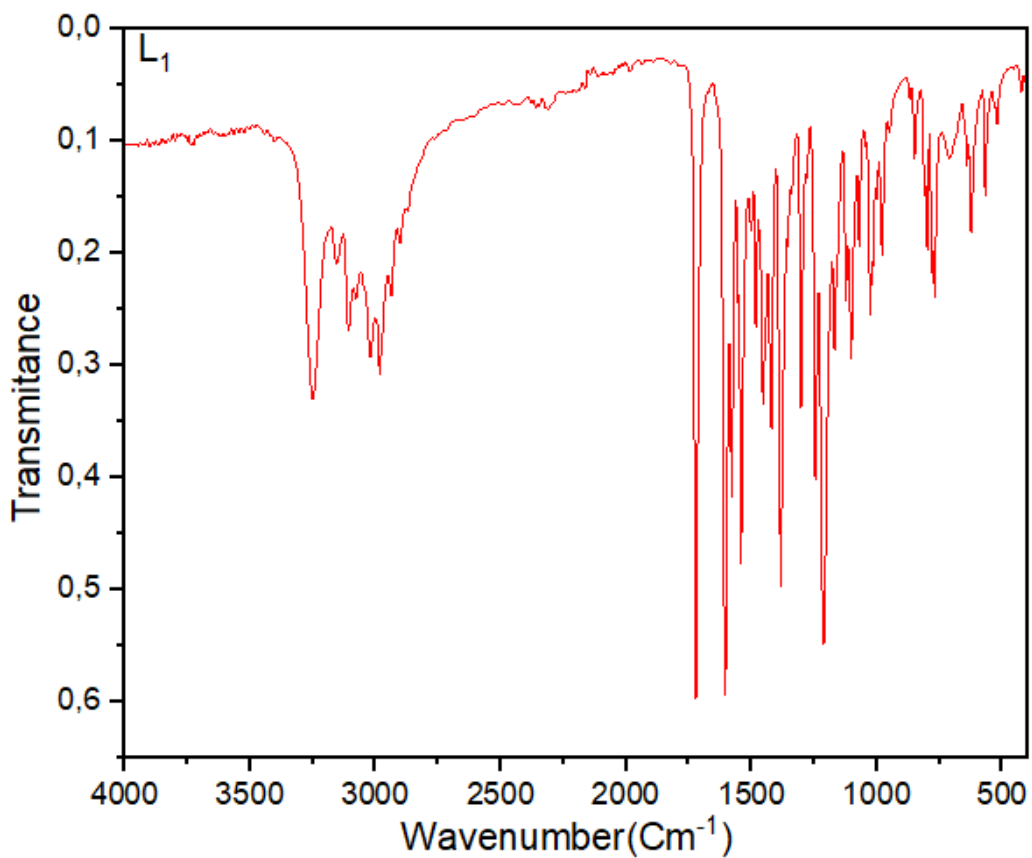


Figure S3. FT-IR spectrum of L_1 .

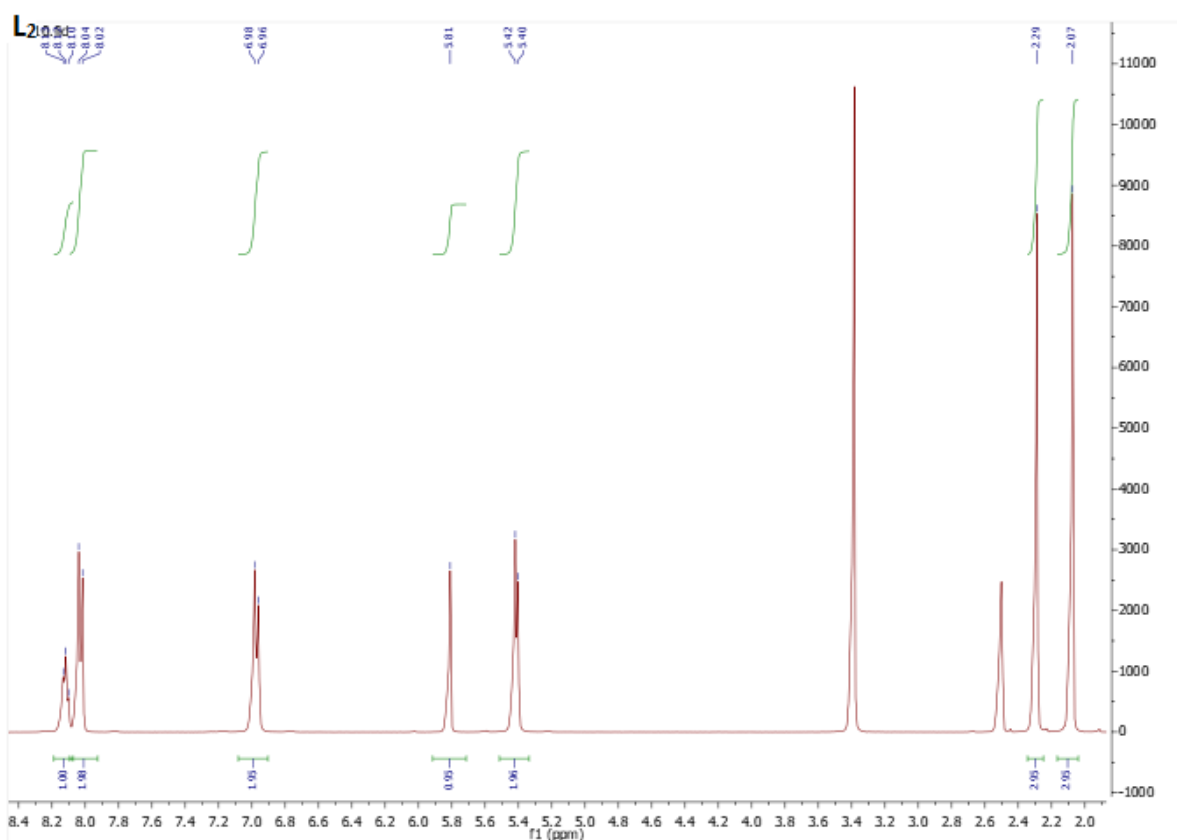


Figure S4. ¹H NMR spectrum of L₂ in DMSO (400 MHz).

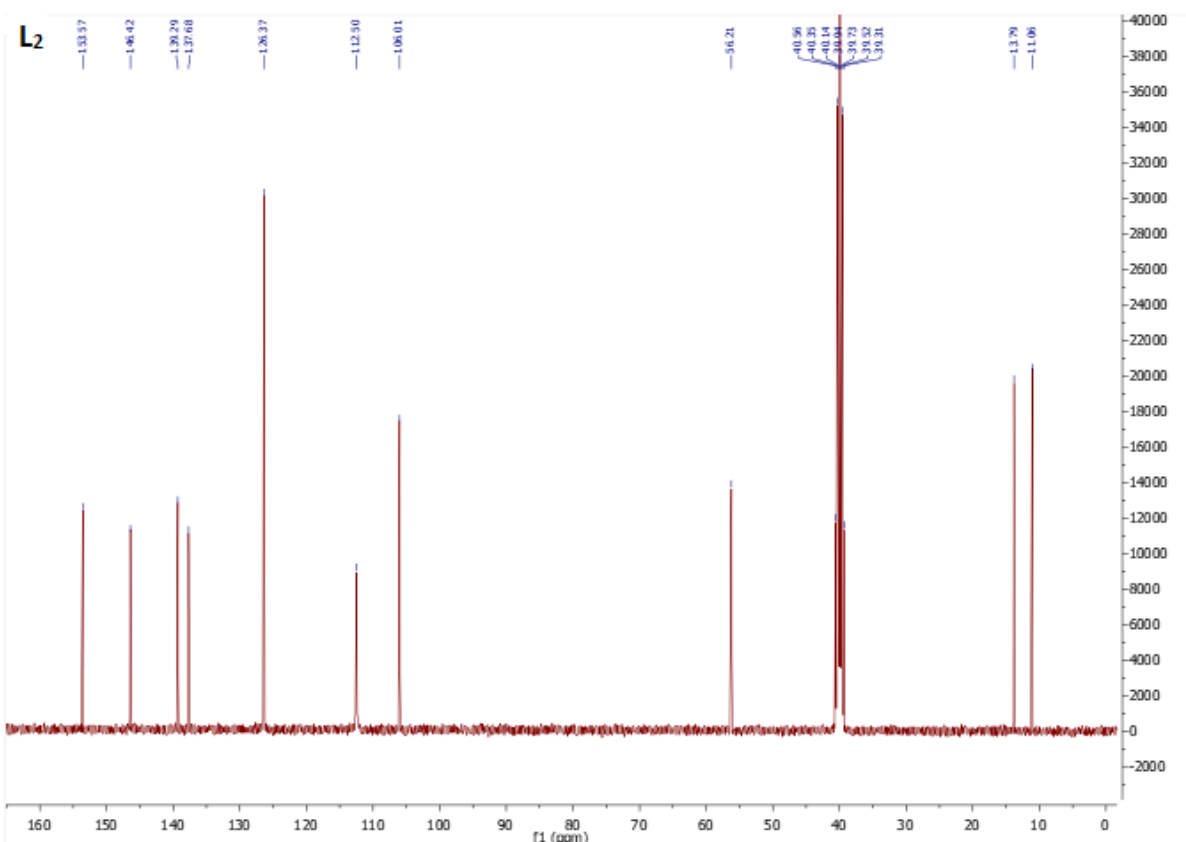


Figure S5. ¹³C NMR spectrum of L₂ in DMSO (400 MHz).

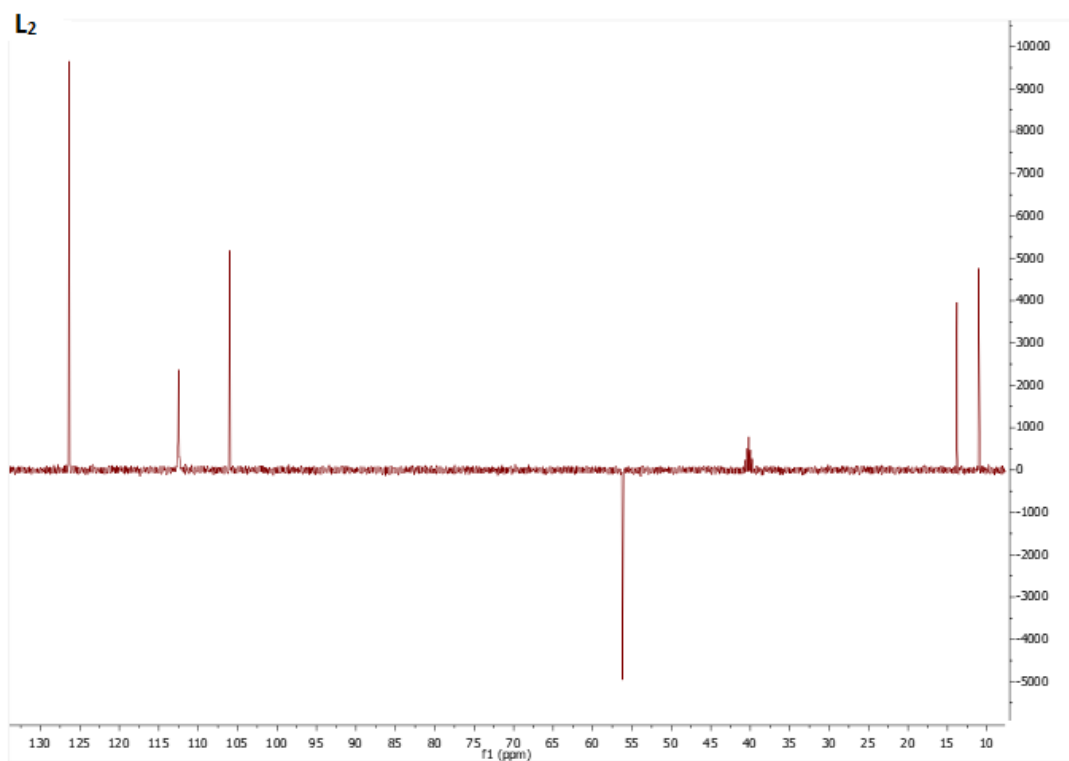


Figure S6. DEPT- 135 NMR spectrum of L_2 in DMSO (400 MHz).

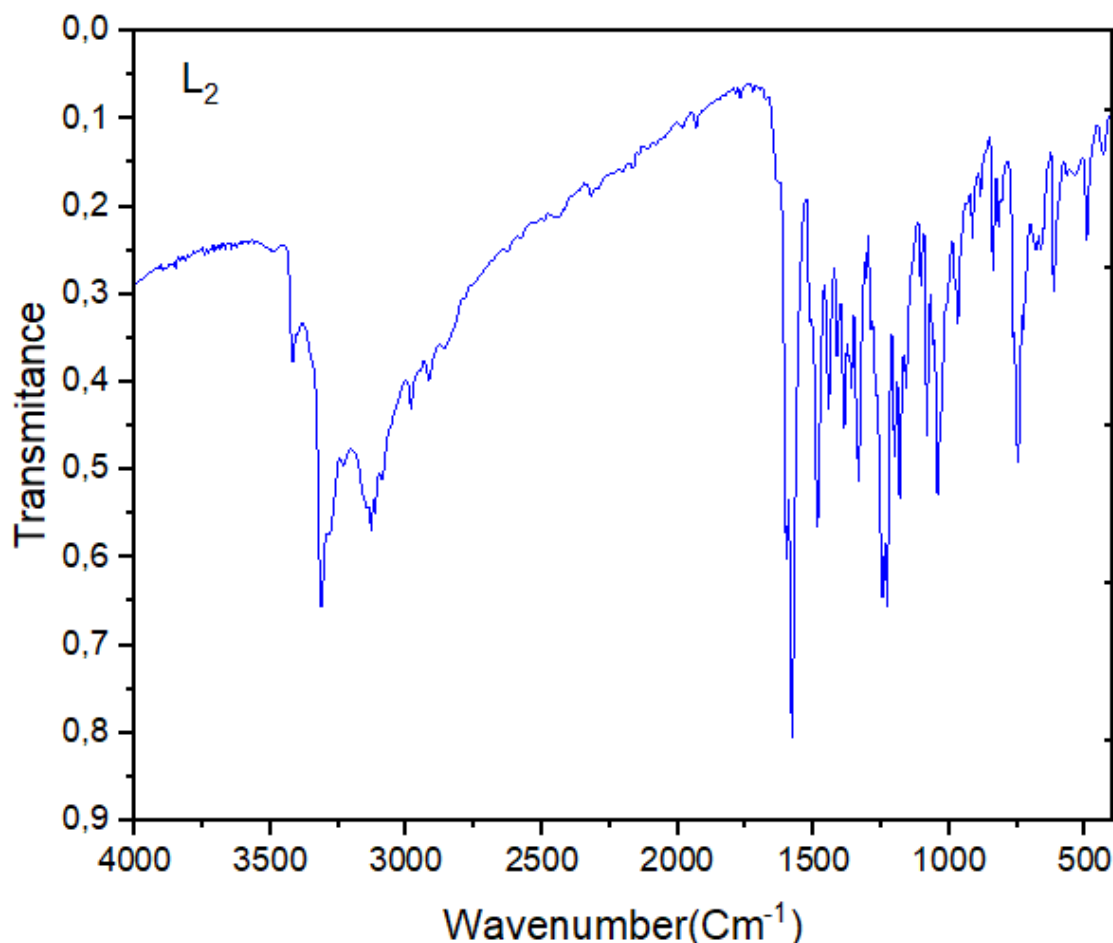


Figure S7. FT-IR spectrum of L_2 .

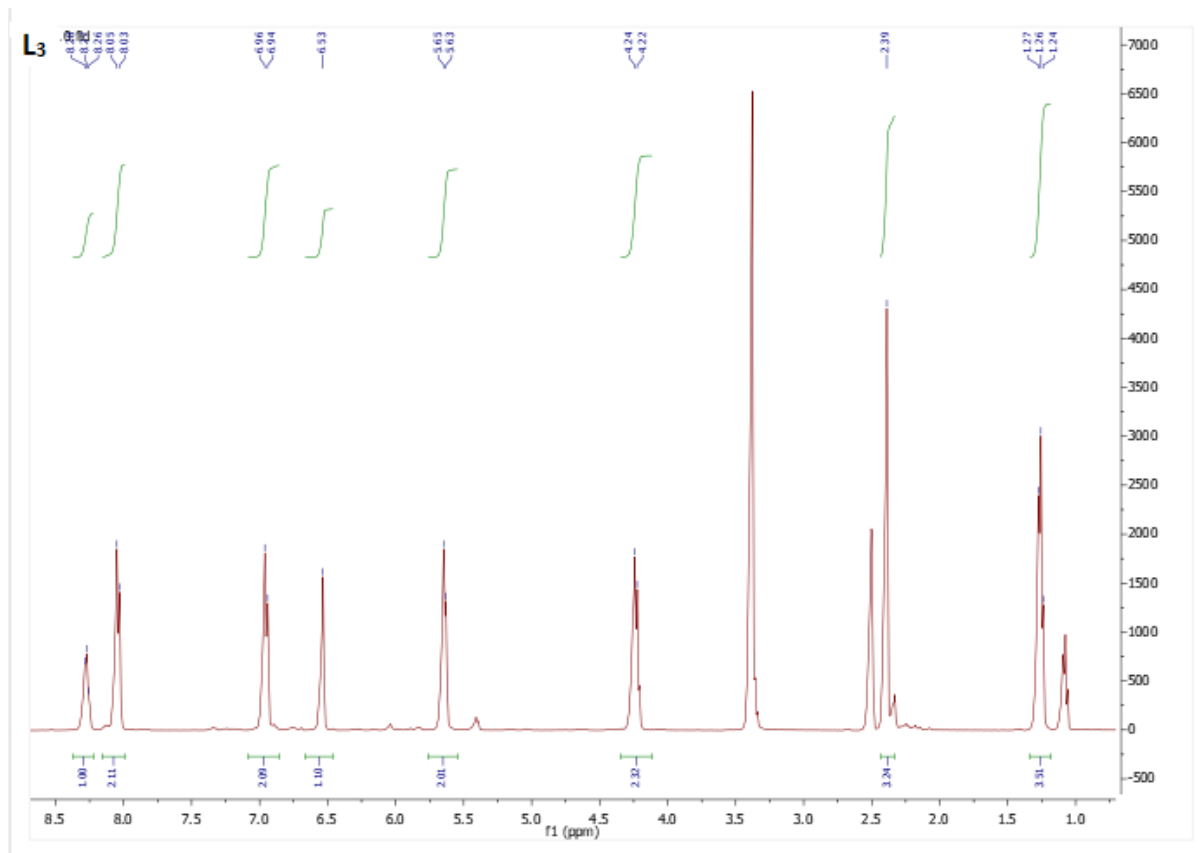


Figure S8. ¹H NMR spectrum of L₃ in DMSO (400 MHz).

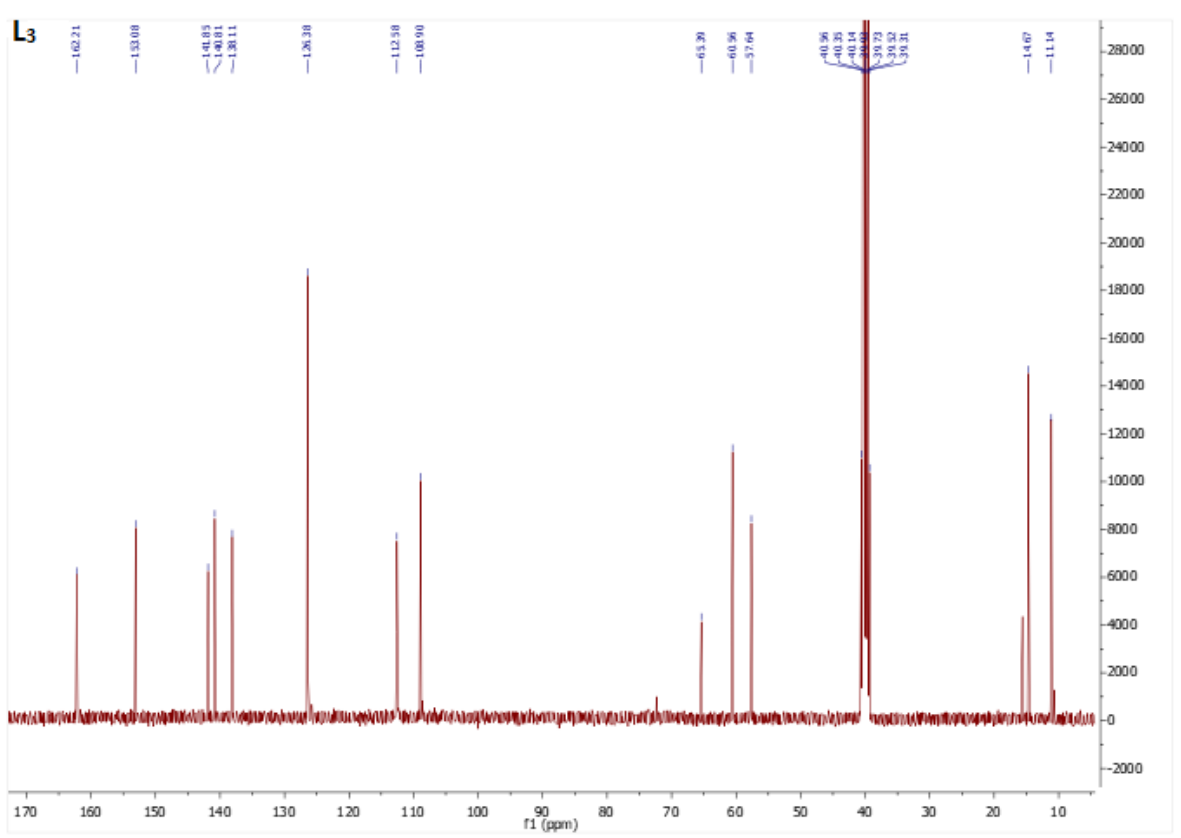


Figure S9. ¹³C NMR spectrum of L₃ in DMSO (400 MHz).

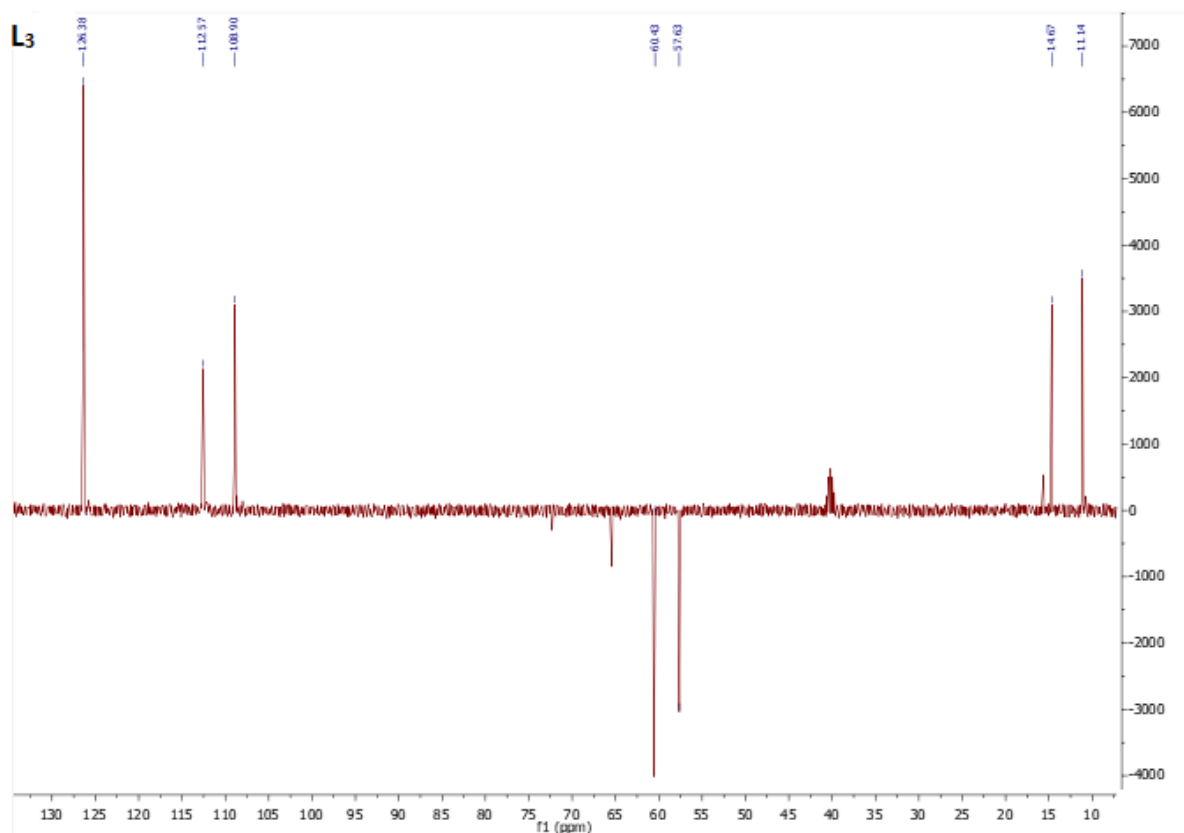


Figure S10. DEPT- 135 NMR spectrum of L_3 in DMSO (400 MHz).

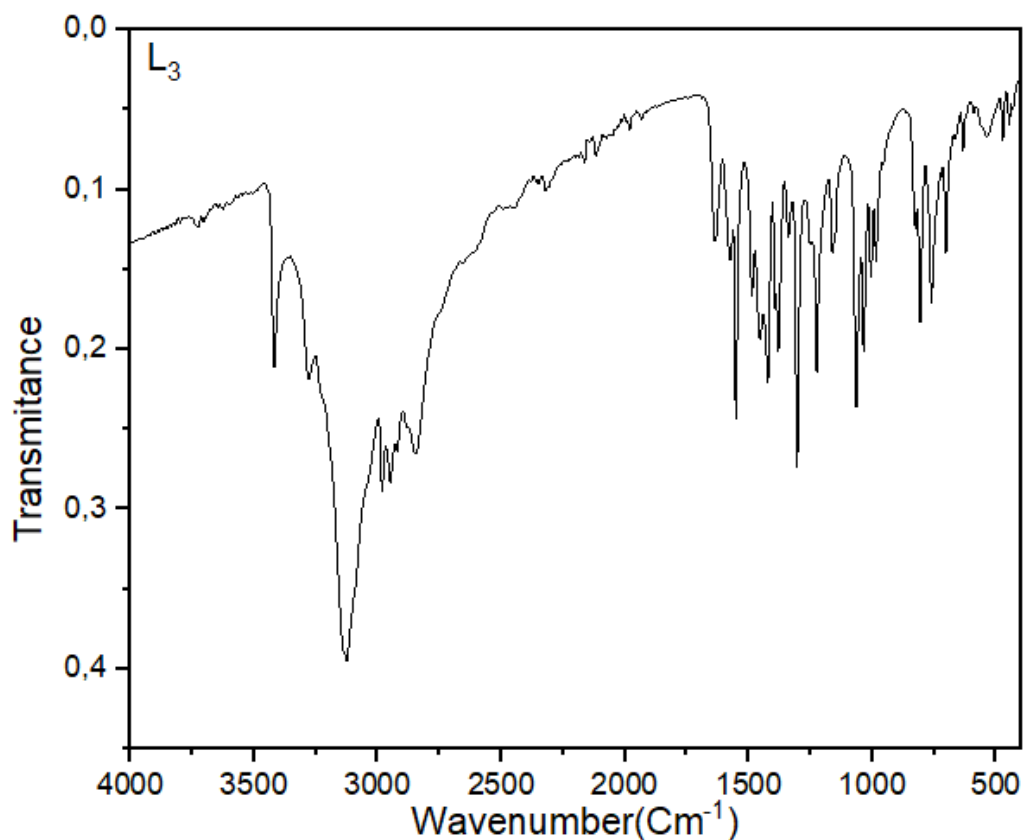


Figure S11. FT-IR spectrum of L_3 .

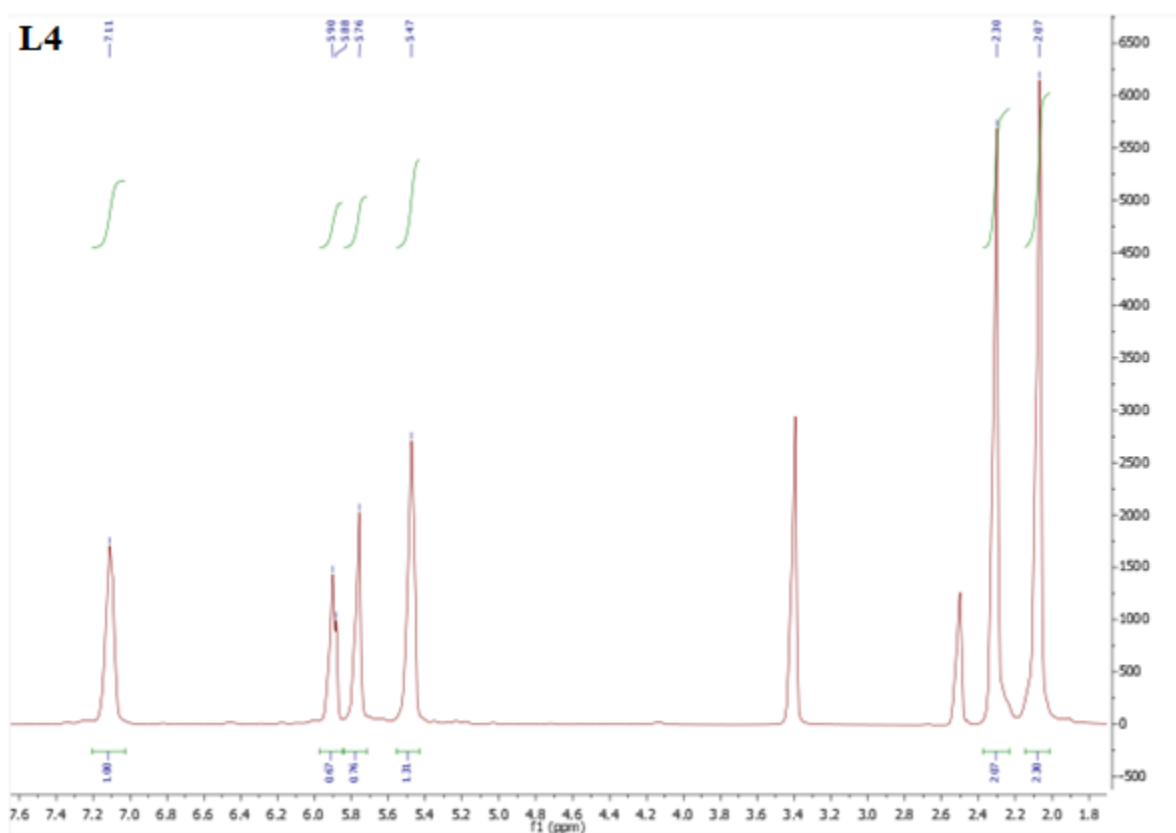


Figure S12. ¹H NMR spectrum of L4 in DMSO (400 MHz).

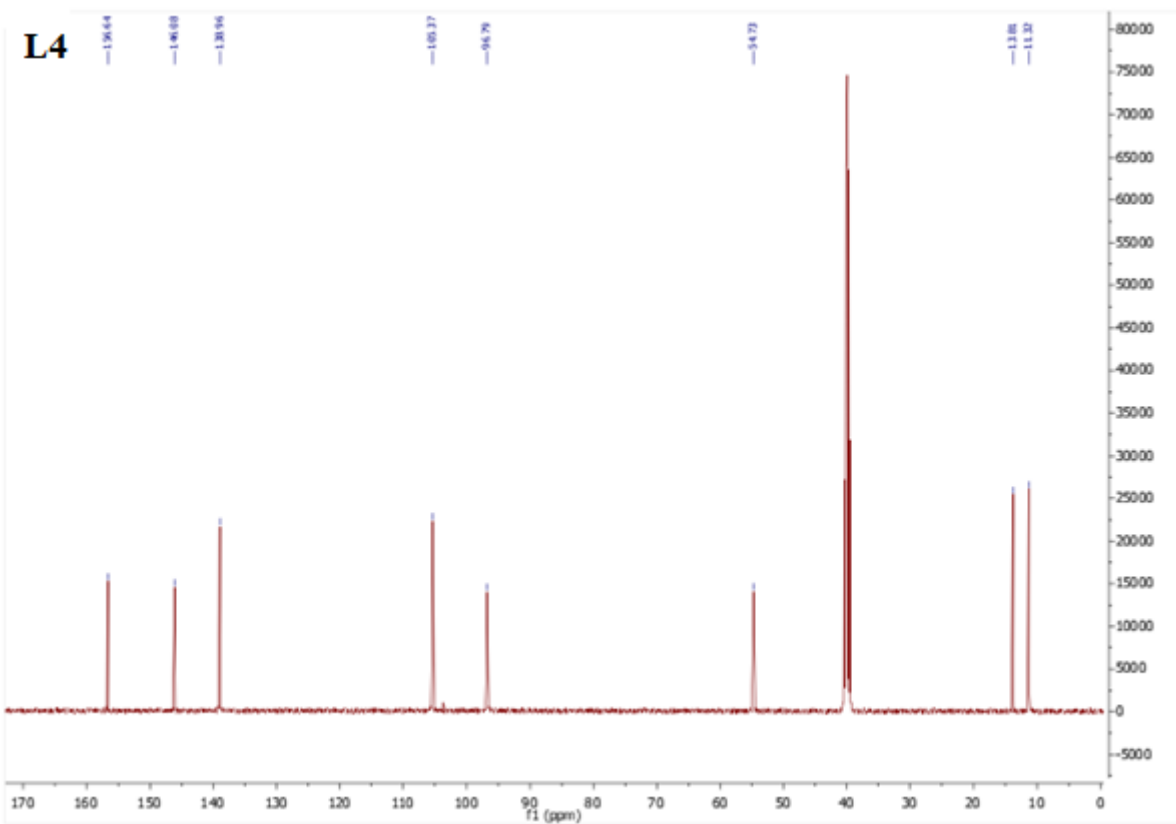


Figure S13. ¹³C NMR spectrum of L4 in DMSO (400 MHz).

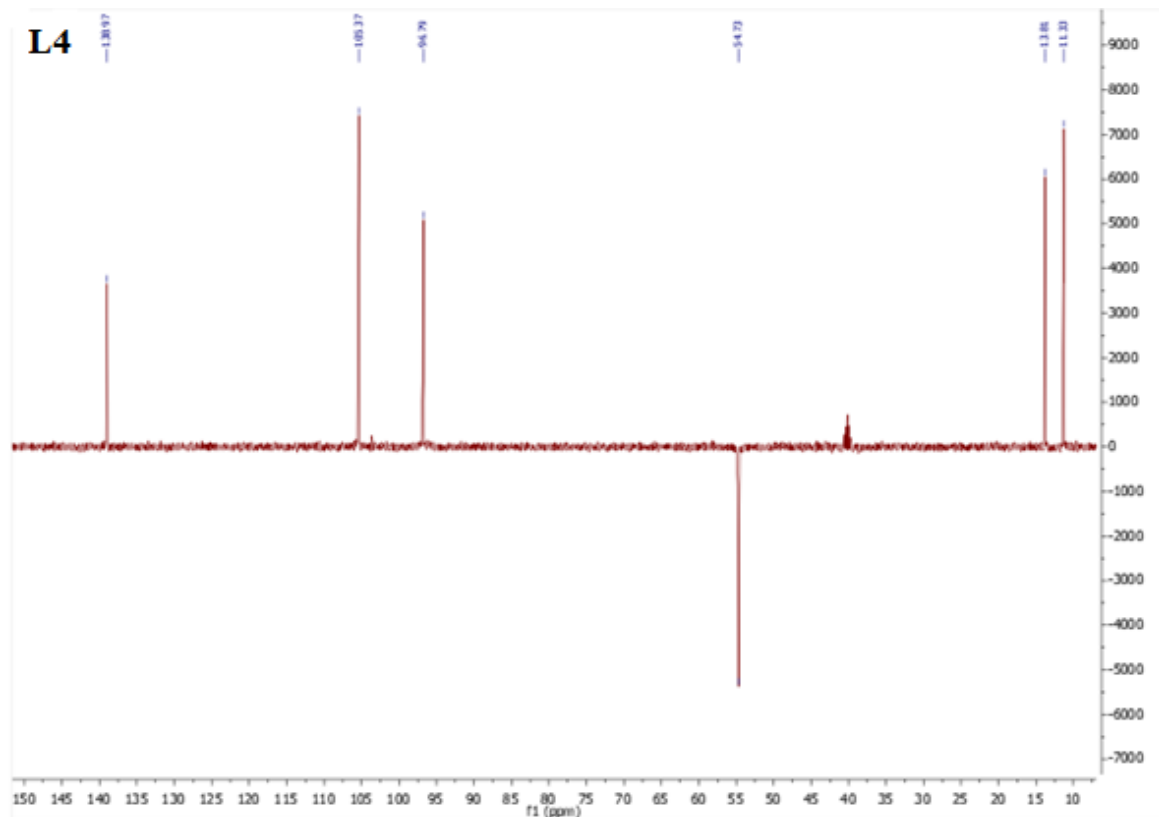


Figure S14. ^{13}C NMR spectrum of L4 in DMSO (400 MHz).

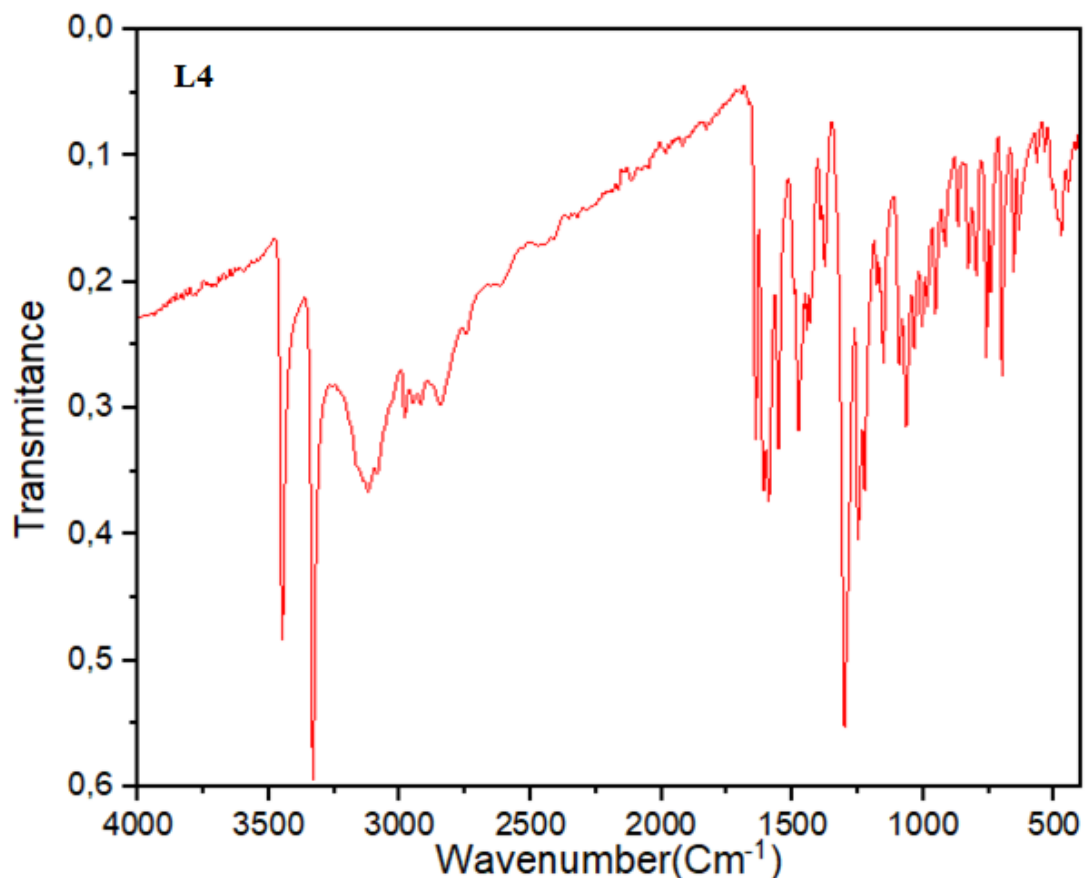


Figure S15. FT-IR spectrum of L4.

2. Effect of concentration

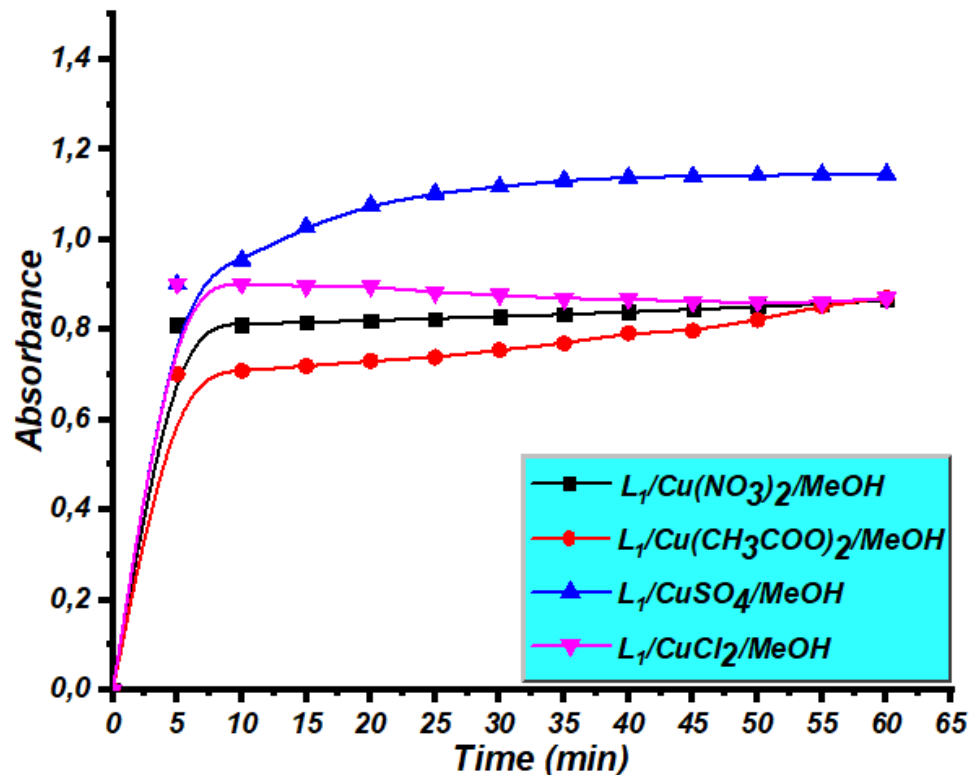


Figure S16. Absorbance evolution of *o*-quinone in presence of complexes formed by L_1 and different copper salts in MeOH.

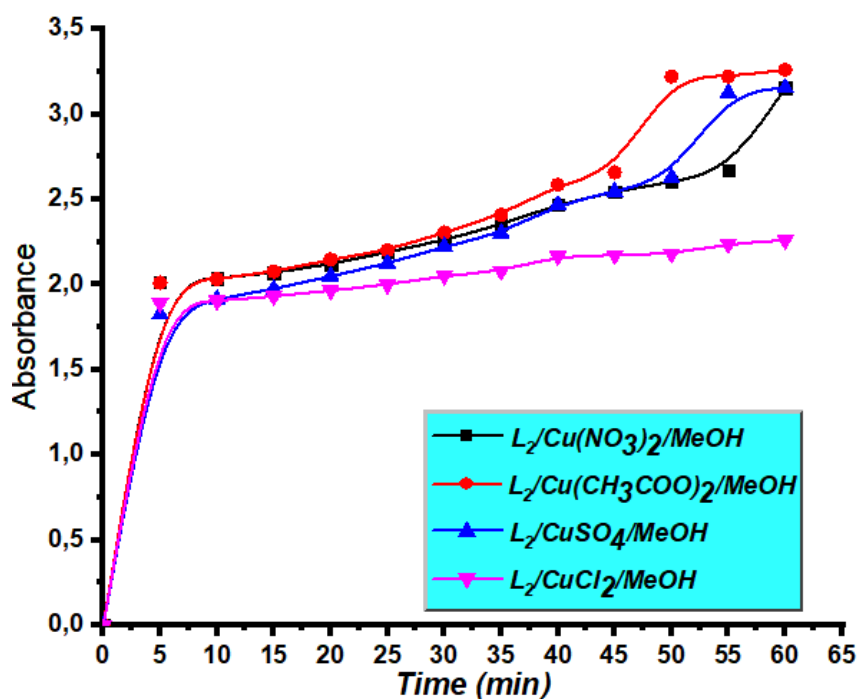


Figure S17. Absorbance evolution of *o*-quinone in presence of complexes formed by L_2 and different copper salts in MeOH.

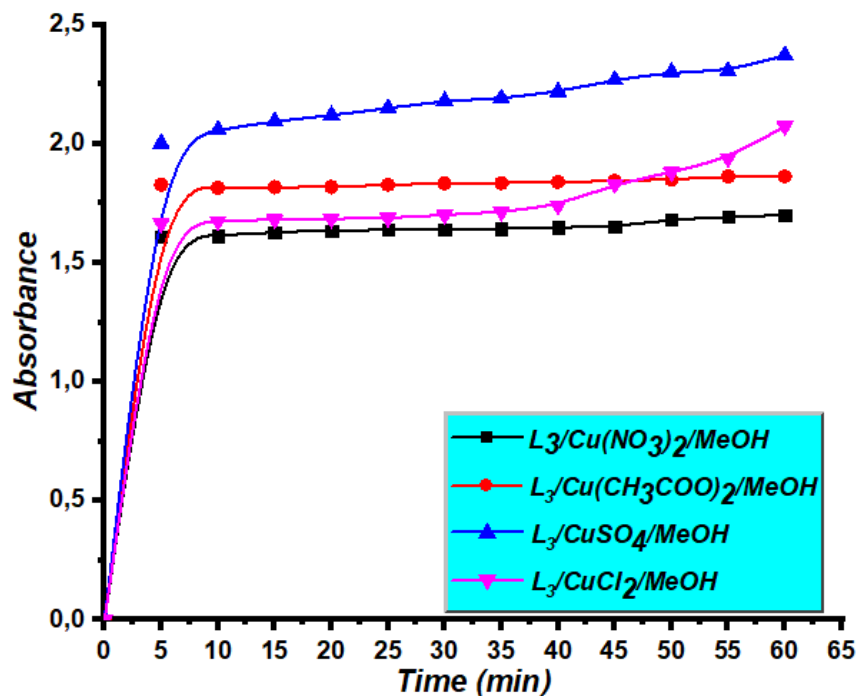


Figure S18. Absorbance evolution of *o*-quinone in presence of complexes formed by L_3 and different copper salts in MeOH.

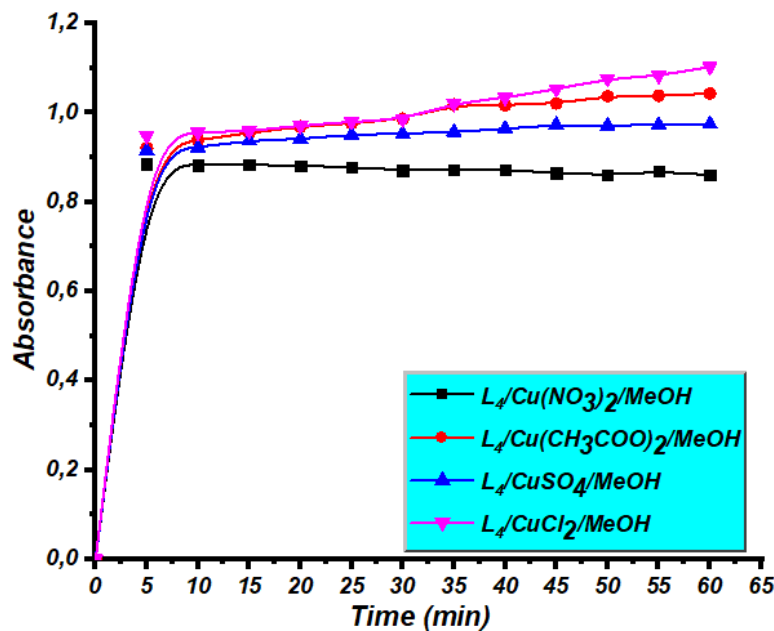


Figure S19. Absorbance evolution of *o*-quinone in presence of complexes formed by L_4 and different copper salts in MeOH.

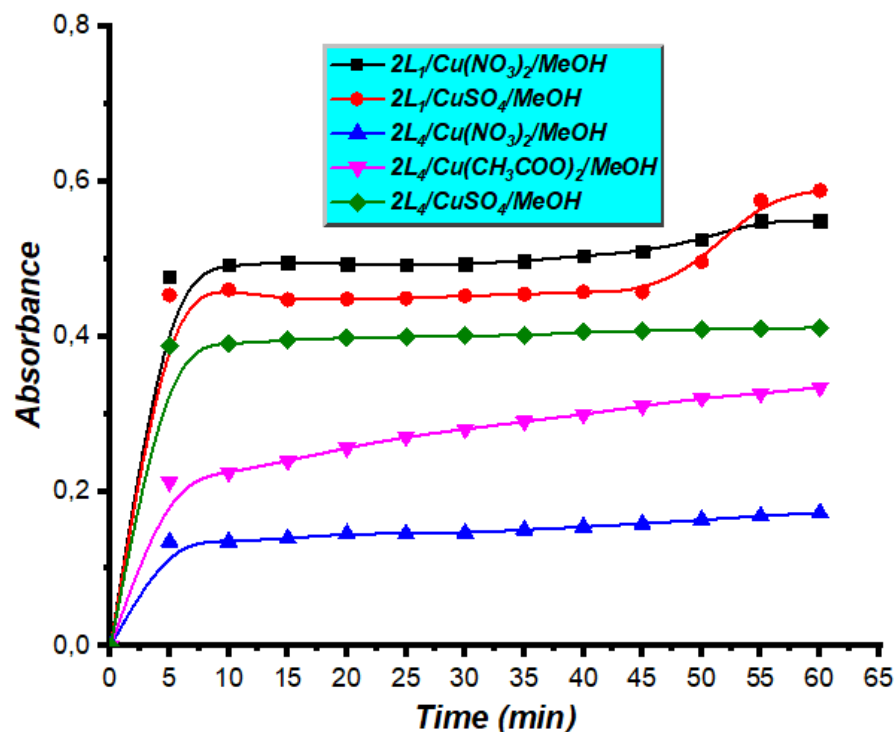


Figure S20. Absorbance evolution of *o*-quinone in presence of complexes formed by \mathbf{L}_1 and \mathbf{L}_4 with different copper salts in MeOH.

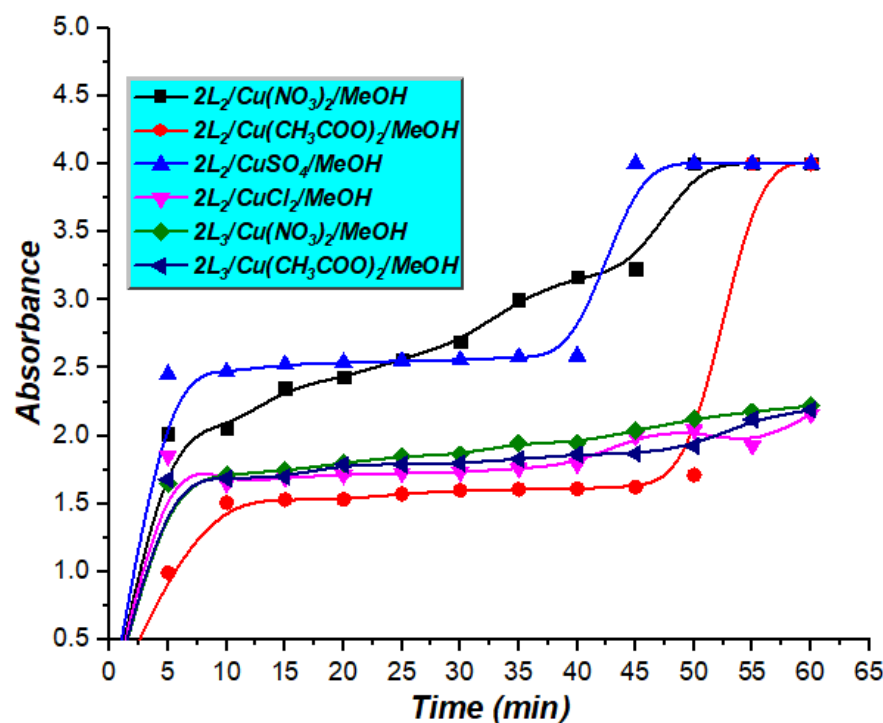


Figure S21. Absorbance evolution of *o*-quinone in presence of complexes formed by \mathbf{L}_2 and \mathbf{L}_3 with different copper salts in MeOH.

3. Solvent effect

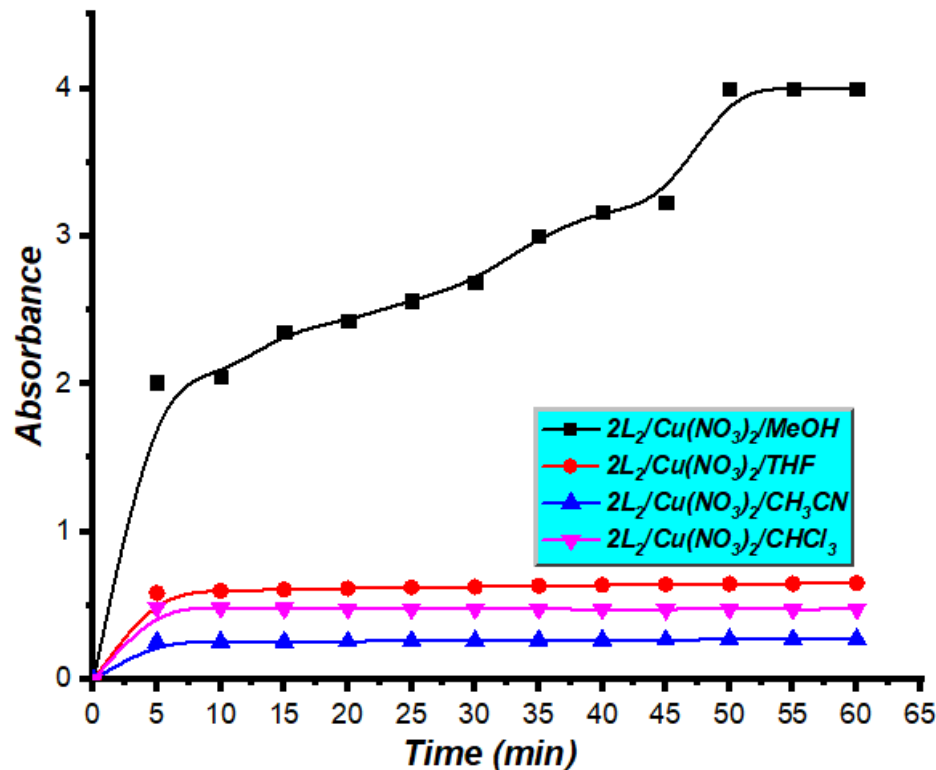


Figure S22. Absorbance evolution of *o*-quinone in presence of complexes formed by $2L_2/Cu(NO_3)_2$ in different solvents.

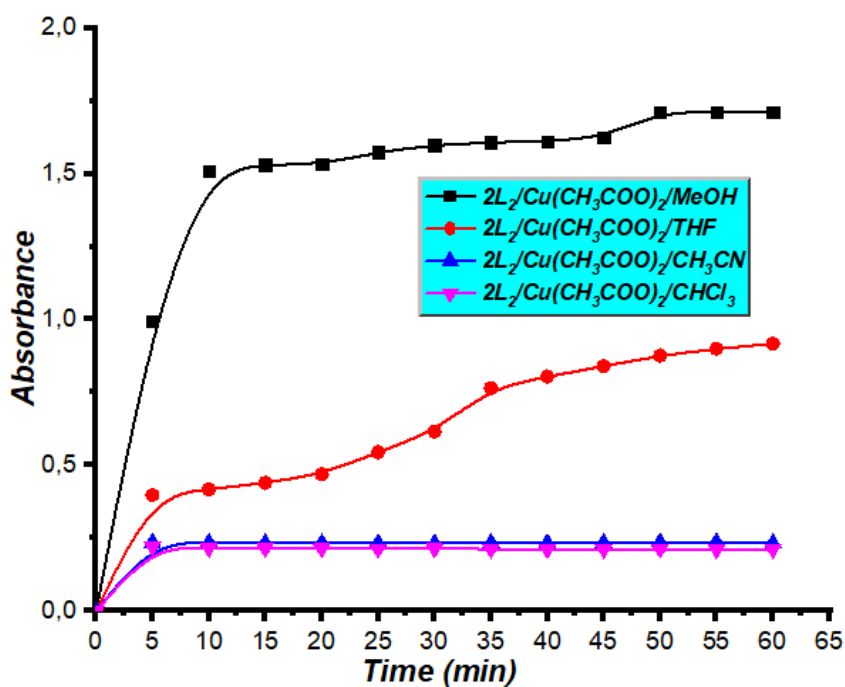


Figure S23. Absorbance evolution of *o*-quinone in presence of complexes formed by $2L_2/Cu(CH_3COO)_2$ in different solvents.

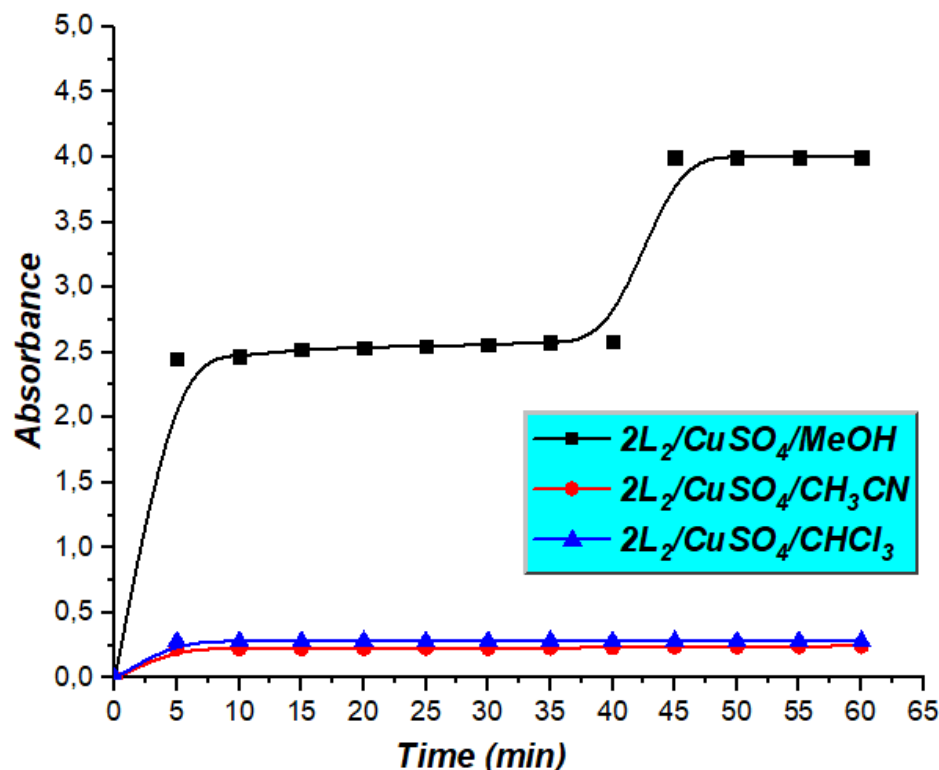


Figure S24. Absorbance evolution of *o*-quinone in presence of complexes formed by $2L_2/\text{CuCuSO}_4$ in different solvents.

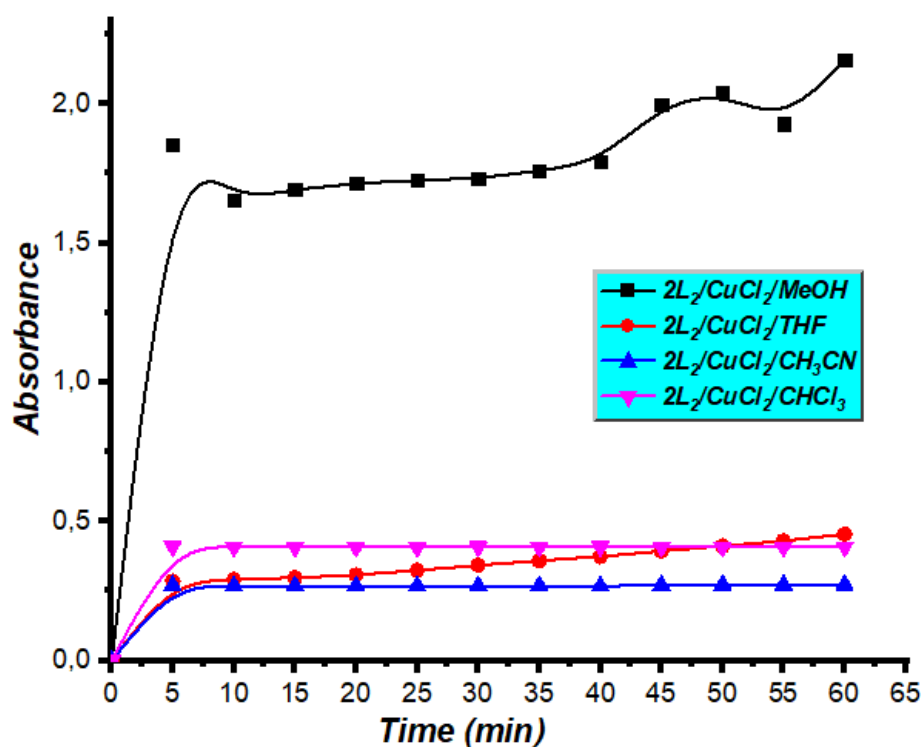


Figure S25. Absorbance evolution of *o*-quinone in presence of complexes formed by $2L_2/\text{CuCl}_2$ in different solvents.

4. Kinetic study

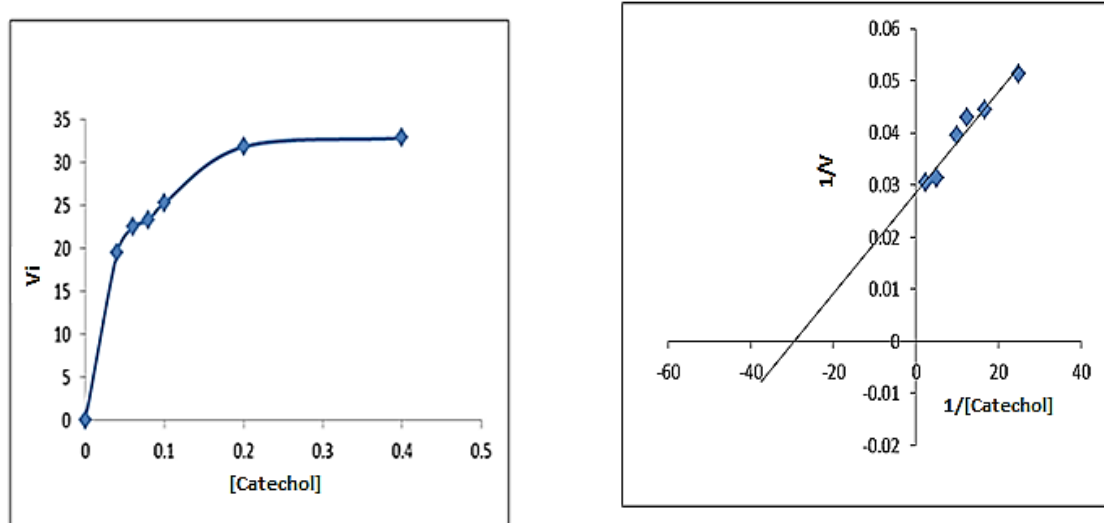


Figure S26. Reaction dependence on the concentration of catechol using $2\text{L}_2/\text{Cu}(\text{NO}_3)_2$.

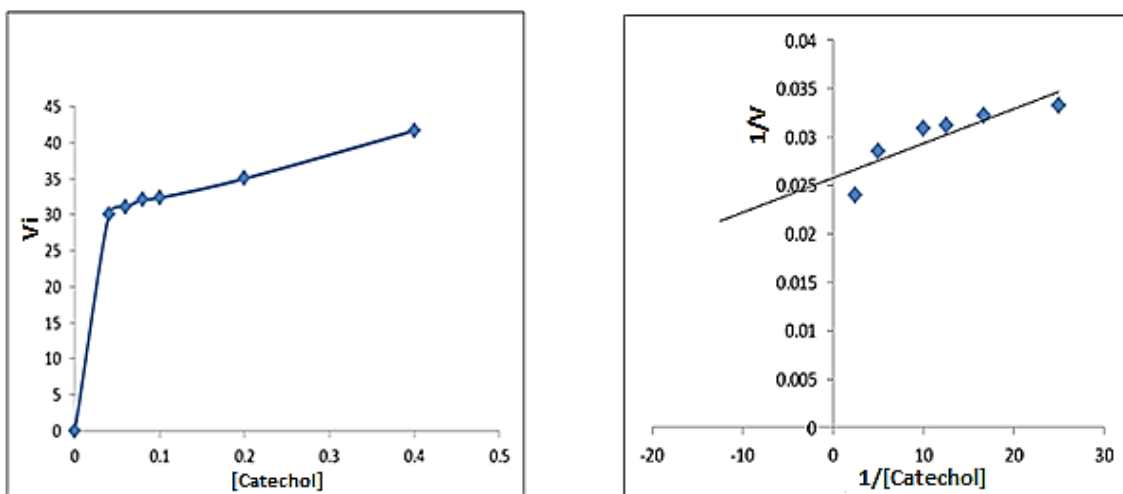


Figure S27. Reaction dependence on the concentration of catechol using $2\text{L}_2/\text{Cu}(\text{CH}_3\text{COO})_2$.

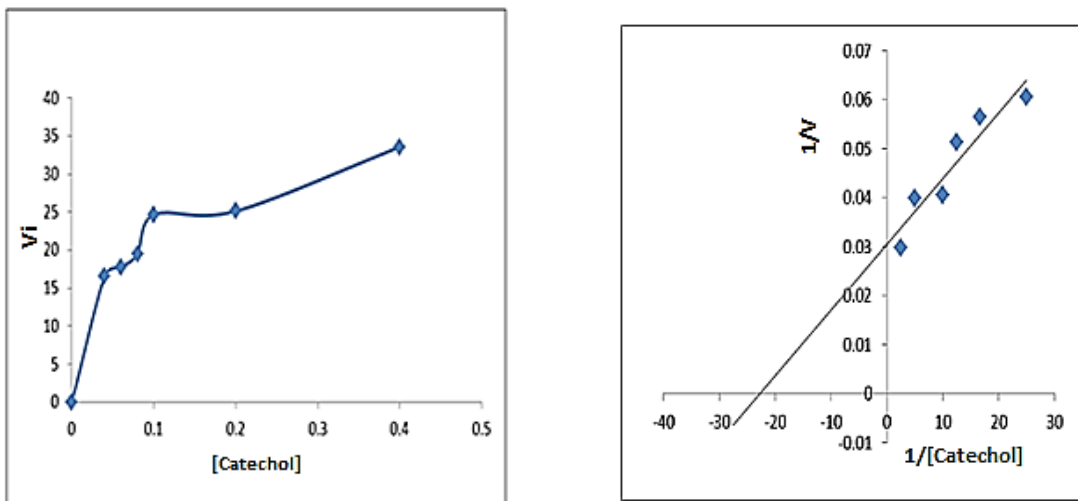


Figure S28. Reaction dependence on the concentration of catechol using $2\text{L}_2/\text{CuSO}_4$.